Solar neutrinos and the principle of equivalence

J. N. Bahcall and P. I. Krastev*
School of Natural Sciences, Institute for Advanced Study, Princeton, New Jersey 08540

C. N. Leung
Department of Physics and Astronomy, University of Delaware, Newark, Delaware 19716
(Received 27 October 1994)

We study the proposed solution of the solar neutrino problem which requires a flavor nondiagonal coupling of neutrinos to gravity. We adopt a phenomenological point of view and investigate the consequences of the hypothesis that the neutrino weak interaction eigenstates are linear combinations of the gravitational eigenstates which have slightly different couplings to gravity, $f_1 G$ and $f_2 G$, $|f_1 - f_2| \ll 1$, corresponding to a difference in redshift between electron and muon neutrinos, $\Delta z/(1+z) \sim |f_1 - f_2|$. Our χ^2 analysis of the available solar neutrino data on observed event rates rules out most of the relevant parameter space, allowing only $|f_1 - f_2| \sim 3 \times 10^{-14}$ for small values of the mixing angle [$2 \times 10^{-3} \lesssim \sin^2(2\theta_G) \lesssim 10^{-2}$] and $10^{-16} \lesssim |f_1 - f_2| \lesssim 10^{-15}$ for large mixing [$0.6 \lesssim \sin^2(2\theta_G) \lesssim 0.9$]. We show that the recoil-electron spectrum measured by the Kamiokande II Collaboration can be used to exclude part of the allowed regions obtained above. We analyze the prospects of using future spectral measurements of solar neutrinos to distinguish the oscillation mechanism due to the violation of the equivalence principle from more conventional mechanisms which require neutrinos to have nondegenerate masses. We find that, for small mixing angles, the flavor nondiagonal coupling to gravity leads to predictions regarding the shape of the ^{8}B-neutrino spectrum which will be distinguishable in the upcoming SNO and Super-Kamiokande experiments and which are independent of solar models.

PACS number(s): 96.60.Kx, 04.80.−y, 12.15.Ff, 14.60.Pq

I. INTRODUCTION

Results from four solar neutrino experiments [1–4] utilizing different detection techniques consistently show a discrepancy between the measured ν_e flux from the sun and the ν_e flux predicted by various solar models [5–13]. Moreover, a comparison of two of the experiments suggests that, essentially independent of solar models, some new physical process may be changing the results of the neutrino energy spectrum [14]. The origin of this solar neutrino deficit is not yet known. A possible solution is neutrino flavor oscillations. One mechanism for neutrino oscillation [15] assumes that neutrinos have nondegenerate masses and that the neutrino mass eigenstates are distinct from their weak interaction eigenstates. We shall refer to this as the mass mechanism. The most often discussed version of this type of solutions is the Mikheyev-Smirnov-Wolfenstein (MSW) effect [16], in which the solar electron neutrinos can be converted almost completely into μ or τ neutrinos due to the presence of matter in the Sun.

An alternative mechanism of neutrino oscillation which does not require neutrinos to have a nonzero mass was first proposed several years ago [17] as a means to test the equivalence principle (EP). In this mechanism, neutrino oscillations occur as a consequence of an assumed flavor nondiagonal coupling of neutrinos to gravity which violates the EP. We shall refer to this as the VEP mechanism.

The VEP mechanism has been studied further in a number of papers [18–21]. One study [20] claims that "current measurements appear to rule out this paradigm" and "a χ^2 analysis associates a confidence level of order 1% or less to the allowed regions." On the other hand, a χ^2 analysis of the data performed in another study [18] reveals regions of the parameter space which are allowed at a higher confidence level by the results of all four solar neutrino experiments. One of our aims in this paper is to find the present status of the VEP mechanism. We repeat the analysis using the most current solar neutrino data and conclude that, although strongly restricted by the data, this mechanism is allowed by the existing data and deserves further study when new experimental data become available.

Having established the VEP mechanism as a possible solution to the solar neutrino problem, it is necessary to find ways to determine whether the mass or the VEP mechanism is responsible for the observed solar neutrino deficit. We show that, because of their differing energy dependence, the two mechanisms yield, in the case of small mixing angles, very different and distinguishable predictions for spectral measurements in future solar neutrino experiments.

*Permanent address: Institute of Nuclear Research and Nuclear Energy, Bulgarian Academy of Sciences, BG–1784 Sofia, Bulgaria.

II. FORMALISM AND SOLUTIONS

We begin by recalling the important features of the two oscillation mechanisms. For simplicity, we only consider mixing of two neutrino flavors: e.g., ν_e and ν_μ. In the mass mechanism, the neutrino weak interaction (flavor) eigenstates $\nu^{(W)} = (\nu_e, \nu_\mu)$ are assumed to be linear superpositions of the mass eigenstates $\nu^{(M)} = (\nu_1^{(M)}, \nu_2^{(M)})$, with a mixing angle θ. The equations describing the evolution of relativistic flavor neutrinos propagating in vacuum are given by

$$i\frac{d}{dr}\begin{pmatrix} A_e \\ A_\mu \end{pmatrix} = \frac{\Delta m^2}{2E}\begin{bmatrix} 0 & \frac{1}{2}\sin 2\theta \\ \frac{1}{2}\sin 2\theta & \cos 2\theta \end{bmatrix}\begin{pmatrix} A_e \\ A_\mu \end{pmatrix}, \quad (1)$$

where E is the neutrino energy, $A_e(r)$ and $A_\mu(r)$ are the probability amplitudes to find an electron or μ neutrino, respectively, at a distance r from the production point of an electron neutrino, $\Delta m^2 \equiv m_2^2 - m_1^2$, and $m_{1,2}$ are the mass eigenvalues. The survival probability for a ν_e after traveling a distance L is

$$P(\nu_e \to \nu_e) = 1 - \sin^2 2\theta \sin^2 \frac{\pi L}{\lambda_M}, \quad (2)$$

where λ_M is the oscillation length defined as

$$\lambda_M = \frac{4\pi E}{\Delta m^2}. \quad (3)$$

In the VEP mechanism neutrinos are assumed to be massless and there is no mass-dependent mixing.[1] Instead the weak interaction eigenstates are assumed to be linear superpositions of the gravitational interaction eigenstates, $\nu^{(G)} = (\nu_1^{(G)}, \nu_2^{(G)})$, with a mixing angle θ_G. It is further assumed that $\nu_1^{(G)}$ and $\nu_2^{(G)}$ interact with gravity with slightly different couplings, thus violating the EP and leading to neutrino oscillations when a neutrino propagates in a gravitational field. The neutrino evolution equations and the survival probability for a ν_e after traversing a distance L in the weak gravitational field of a static, spherical symmetric source are given (in the harmonic gauge) by Eqs. (1) and (2), with the substitutions [17]

$$\theta \to \theta_G \quad \text{and} \quad \frac{\Delta m^2}{2E} \to 2E|\phi(r)|\Delta f, \quad (4)$$

where $\phi(r)$ is the Newtonian gravitational potential and $\Delta f \equiv f_2 - f_1$ is a measure of the degree of EP violation. Here $f_{1,2}$ can be identified as parameters in the parametrized post-Newtonian formalism [22,23], and $f_1 = f_2$ if the EP is obeyed. In general relativity, $f_1 = f_2 = 1$.

There has been much discussion in the literature [24], mostly in the context of testing the EP in the K^0-$\overline{K^0}$ system, as to whether the gravitational potential in Eq. (4) should include the potential of matter other than the Sun. If distant matter is included, then one obtains the counterintuitive result that the biggest effect is from material far away from the solar system. We adopt here the phenomenological point of view that the relevant potential $\phi(r)$ is the difference between the Newtonian potential of the solar material at r and at $r = \infty$.

It is conceivable that the description of the violation of the equivalence principle outlined above will be modified if the violation is derived from a more rigorous theory, e.g., from string theory [25]. The dependence on the gravitational potential might be replaced in such a theory by a dependence on the gradient of the potential, which would eliminate the above-mentioned ambiguity concerning the relevant gravitational potential. For example, the term in Eq. (4) may be replaced by

$$2E|\phi(r)|\Delta f \to ER_f|\nabla\phi|, \quad (5)$$

where R_f is a dimensional parameter that describes the violation of the equivalence principle. The results obtained below for the VEP mechanism as defined in Eq. (4) can be easily translated to the case represented by Eq. (5). Since $|\nabla\phi| \sim R_\odot^{-1}|\phi|$, where $R_\odot$ is the solar radius, we can interpret the numerical results for Δf in Eq. (4) as constraints on a mass scale related to flavor violation:

$$M_f \simeq (R_\odot \Delta f)^{-1}. \quad (6)$$

The allowed range of this mass scale is $10^{-2} - 1$ eV, the lower end of which coincides with the relevant mass scale for the adiabatic MSW solution of the solar neutrino problem.

It follows from the substitution (4) and Eq. (3) that the oscillation length in the VEP mechanism is, for a constant gravitational potential,

$$\lambda_G = \frac{\pi}{E|\phi|\Delta f}. \quad (7)$$

Notice that λ_G is inversely proportional to the neutrino energy, whereas λ_M increases with E. It is this different energy dependence that leads to the observable distinction between the VEP and mass mechanisms.

Another consequence of this differing energy dependence is that, in contrast with the mass mechanism, the VEP mechanism cannot account for the observed solar neutrino deficit as the result of long-wavelength vacuum oscillations [18]. On the other hand, the solar neutrino data can be explained in terms of the VEP mechanism by invoking also the mechanism of resonance enhanced transitions in the Sun. For neutrinos propagating in matter, the evolution equations, Eq. (1), for the mass (VEP) mechanism are modified such that

$$\cos 2\theta_{(G)} \to \cos 2\theta_{(G)} - \frac{\sqrt{2}G_F N_e(r)}{2\pi/\lambda_{M(G)}}, \quad (8)$$

where G_F is the Fermi constant and $N_e(r)$ is the electron

[1] We do not consider explicitly the case of massive neutrinos in the VEP mechanism (see, however, Appendix A) because this just complicates the analysis by introducing more parameters, but does not change significantly the limits that are derived. See Ref. [21] for a recent discussion of this case.

number density inside the Sun. In the VEP case, the resonance occurs when

$$E = \frac{\sqrt{2}G_F N_e(r)}{2|\phi(r)|\Delta f \cos 2\theta_G}. \quad (9)$$

An important ingredient in the analysis of resonant transitions in the Sun is the adiabaticity condition. For the VEP mechanism, it reads

$$\kappa = \frac{\sqrt{2}G_F\,(N_e)_{\rm res}\tan^2 2\theta_G}{\left|\left(\frac{1}{N_e}\frac{dN_e}{dr}\right) - \left(\frac{1}{\phi}\frac{d\phi}{dr}\right)\right|_{\rm res}} \gg 1. \quad (10)$$

For the mass mechanism, simply drop the $\phi^{-1}d\phi/dr$ term in the denominator and replace θ_G by θ. The dependence on the energy is implicit as the energy determines the resonant density via Eq. (9). Note that the adiabaticity condition in the VEP case is violated for low energy neutrinos whereas it is violated in the mass mechanism for high energy neutrinos. A general discussion of the adiabaticity condition in the VEP mechanism which is valid also for massive neutrinos is given in Appendix A.

It can be shown from Eqs. (1) and (8) that the probability amplitude $[A_e(r)]$ of finding an electron neutrino at a distance r from where it was produced satisfies the equation

$$A_e'' + A_e'(ia - b'/b) + b^2 A_e = 0, \quad (11)$$

where the primes denote derivatives with respect to r. The parameters a and b are defined as

$$a = -\sqrt{2}G_F N_e(r) - 2E\phi(r)\Delta f \cos 2\theta_G, \quad (12)$$

$$b = -E\phi(r)\Delta f \sin 2\theta_G. \quad (13)$$

Equation (11) is exactly solvable in the case of a Newtonian gravitational potential and zero electron density (e.g., outside the Sun). The general solution, expressed in terms of the dimensionless variable, $x = r/R_\odot$, has the form

$$A_e(x) = C_1 x^{iS\cos^2\theta_G} + C_2 e^{i\omega} x^{-iS\sin^2\theta_G}, \quad (14)$$

where C_1, C_2, and ω are real constants that have to be determined by the initial conditions. For a neutrino moving in the gravitational potential of the Sun, $S = 2E\Delta f G_N M_\odot$, where G_N is Newton's gravitational constant and $M_\odot$ is the solar mass. The probability to find a ν_e at a distance x, if at $x = 1$ a ν_e has been produced, is thus

$$P(x) = 1 - \sin^2(2\theta_G)\sin^2\left(\frac{S}{2}\ln(x)\right), \qquad x \geq 1. \quad (15)$$

By analogy with neutrino oscillations in vacuum one can introduce the oscillation length, $L_G = 2\pi x R_\odot/S\ln(x)$, which turns out to be distance dependent. From (14) one can derive the average probability to obtain an electron neutrino at infinity given an arbitrary neutrino state at $r = R_\odot$:

$$\bar{P} = \cos^2 2\theta_G P(1) - \sin 2\theta_G \cos 2\theta_G R(1) + \frac{1}{2}\sin^2 2\theta_G. \quad (16)$$

Here $R(1) = \mathrm{Re}[A_e(1)A_\mu^*(1)]$. This expression is necessary for the computation of the mean survival probabilities, especially in the case of large mixing angles, $\sin^2 2\theta_G \geq 0.1$, where one has to average over large-amplitude oscillations in vacuum between the Sun and the Earth. It is important also for the analysis in the long-wavelength regime where the oscillation length becomes comparable to the Earth-Sun distance. We have used these results to verify the finding in [18] that the possibility of a long-wavelength (or "just-so") VEP solution to the solar neutrino problem is ruled out by the present data. The main reason for this is the inverse energy dependence of the oscillation length. In order to reconcile the data from all four detectors the boron neutrinos have to be suppressed by about 50% and the lower energy ^{7}Be neutrinos have to be suppressed even more. When Δf is chosen such that the oscillation length of the boron neutrinos, which give the biggest contribution to the signal in the chlorine detector, is approximately twice the distance between the Sun and the Earth, the lower energy neutrinos, because of their longer oscillation length, will be suppressed less, which contradicts the data.

The survival probability as a function of the product $E\Delta f$ is shown in Fig. 1 for a small as well as a large mixing angle. The curves in Fig. 1 have been obtained after averaging over the neutrino production regions [5] of the different components of the solar neutrino flux. The survival probabilities have been computed using the analytical result (see Appendix B)

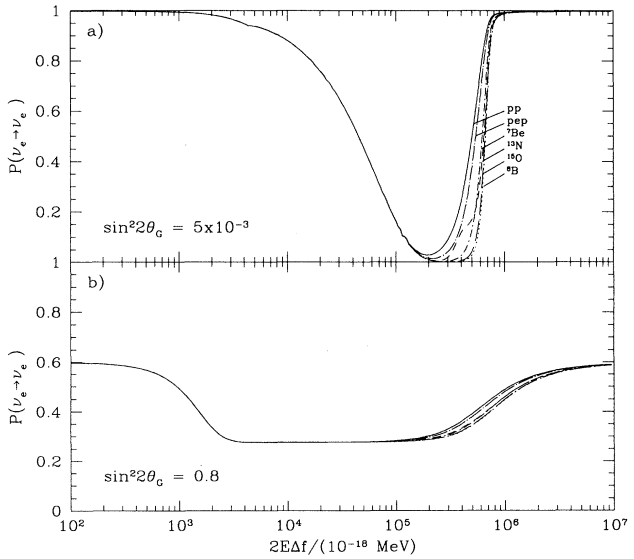

FIG. 1. Survival probabilities as a function of $E\Delta f$ for (a) $\sin^2 2\theta_G = 5\times10^{-3}$ and (b) $\sin^2 2\theta_G = 0.8$. The different curves correspond to averaging over the different neutrino production regions according to the solar model in [5].

$$P = \frac{1}{2} + \left(\frac{1}{2} - P_{LZ}\right) \cos 2\theta_G^{\circ} \cos 2\theta_G, \qquad (17)$$

where $P_{LZ} = (e^{-\beta} - e^{-\alpha})/(1 - e^{-\alpha})$, with $\alpha = 2\pi\kappa \cos 2\theta_G / \sin^2 2\theta_G$ and $\beta = \frac{\pi}{2}\kappa(1 - \tan^2\theta_G)$. Here θ_G° is the mixing angle at the production point of the neutrino. These expressions have been obtained by analogy with the ones in [26] for MSW transitions in the mass mechanism. It is exact in the case of a density which varies exponentially with the distance r assuming that the variation of the gravitational potential with distance is much slower than the variation of the density with distance and can be neglected altogether. For small mixing angles this is an excellent approximation as the scale height of the gravitational potential is much larger than the density scale height. For example, the gravitational potential changes by a factor less than 10 from the center of the Sun to the surface whereas the density changes by several orders of magnitude. We use the density distribution inside the Sun as given in [5] both for the electron number density and to compute the gravitational potential, inside the Sun. For each value of $E\Delta f$ the electron number density, the gravitational potential, and their logarithmic derivatives have been put equal to the corresponding values they assume at the point where the resonance takes place. We have verified by numerical integration of the evolution equations that the analytical results obtained with Eq. (17) are accurate to a few percent.

Despite the superficial similarity between the shapes of the suppression curves in the VEP and in the mass mechanism there are some important differences between these two cases. In contrast with the mass mechanism, the adiabatic edge of the suppression pit in the case of VEP is at higher energies, whereas the nonadiabatic edge is at lower energies. The position of the adiabatic edge is bounded by the maximal density in the Sun ($\approx 100 N_A$ cm^{-3}) to be at $E\Delta f \approx 10^{-12}$ MeV. The nonadiabatic edge shifts toward higher $E\Delta f$ with decreasing mixing angle in accordance with the adiabaticity condition, Eq. (10).

The resonance and adiabaticity conditions together determine the range of parameters which can be probed by solar neutrino experiments. This is depicted in Fig. 2 as the region bounded by the dotted lines. The horizontal line corresponds to a resonant density equal to the density in the center of the Sun for neutrinos with energy 0.2 MeV. For $\Delta f > 2 \times 10^{-12}$ there will be no resonance crossing in the Sun for neutrinos with energies higher than 0.2 MeV. Oscillations with an amplitude $\sim \sin^2 2\theta_G$ will still take place, however, the oscillation length at the Earth for neutrinos of energies 0.2 MeV and higher will be smaller than $10^{-1} R_{\odot}$. Therefore the averaging over the distance between the source and detector will eliminate the oscillating term which will result in an energy-independent suppression of all solar neutrino fluxes. The latter does not give an acceptable fit to the data. The diagonal line in Fig. 2 corresponds to $\kappa = 1$ for neutrinos of energy 10 MeV. For values of $\sin^2 2\theta_G$ and Δf in the region below this line the transitions are strongly nonadiabatic and cannot account for the solar neutrino problem.

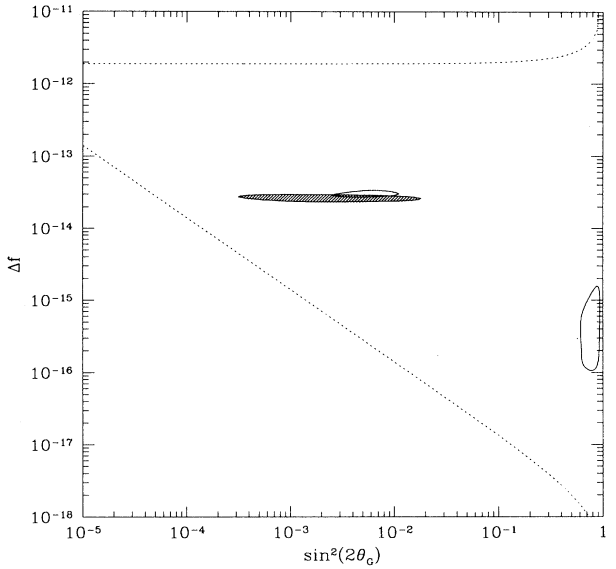

FIG. 2. 95% C.L. allowed regions of the parameters Δf and $\sin^2 2\theta_G$ derived from the latest solar neutrino data (unhatched). The region that can be probed with solar neutrino experiments is bounded by the dotted lines. The hatched region is ruled out by the recoil-electron energy spectrum measured by the Kamiokande II Collaboration.

III. COMPARISON WITH DATA

In Sec. III A we show which regions of the parameter space for the VEP mechanism are ruled out by the measured counting rates in the four operating solar neutrino experiments. In Sec. III B we use the implied spectral distribution of the ^{8}B-neutrino spectrum and the existing Kamiokande measurements to further reduce the allowed parameter space. We also show in Sec. III B, and especially Figs. 3 and 4, how future spectral measurements with SNO and Super-Kamiokande can be used to distinguish between different mechanisms for solving the solar neutrino problem.

A. Rates

We use the following recent experimental results: $Q_{\rm Cl} = (2.55 \pm 0.25)$ solar neutrino units (SNU) [1], $\Phi_K(^8\mathrm{B}) = (2.89 \pm 0.41) \times 10^6$ cm^{-2}s^{-1} [2], $Q_{\rm Ga} = (73 \pm 18.7)$ SNU [3], and $Q_{\rm Ga} = (79 \pm 11.7)$ SNU [4].

In our χ^2 analysis of the latest solar neutrino data in terms of the "MSW-enhanced" VEP mechanism we have adopted a procedure that takes into account the theoretical uncertainties in the standard solar model as described in [27]. The analysis yields two allowed regions at 95% C.L.: a "small mixing region" for $2 \times 10^{-3} \leq \sin^2(2\theta_G) \leq 10^{-2}$ and $2.7 \times 10^{-14} \leq \Delta f \leq 3.3 \times 10^{-14}$; and a "large mixing region" for $0.6 \leq \sin^2(2\theta_G) \leq 0.9$ and $1.0 \times 10^{-16} \leq \Delta f \leq 1.5 \times 10^{-15}$. These are shown in Fig. 2 by the unhatched regions within the solid curves. The quality of the fit is better for the small mixing solution

where $\chi^2_{\rm min} = 0.31$. For two degrees of freedom (four experiments, two parameters fitted), this is a very good fit comparable to the case of the MSW solution in the mass mechanism where $\chi^2_{\rm min} = 0.12$ (see [28]). For the large mixing angle solution the fit is considerably worse with $\chi^2_{\rm min} = 3.4$. The allowed regions shown in Fig. 2 are compatible with the ones found in [18]. The differences can be attributed to the more recent experimental data used in the present analysis as well as to the different ways in which these data were treated.

We have repeated our analysis of the data by including the gravitational field of the local supercluster which is estimated by Kenyon [24] to be 3×10^{-5}. This potential, being three times the gravitational potential of the Sun at its center, would dominate. The allowed regions in this case change little in shape but are shifted to lower values of Δf by approximately a factor of 3. The small mixing allowed region is shifted also to smaller angles $[1.5 \times 10^{-3} \leq \sin^2(2\theta_G) \leq 6.0 \times 10^{-3}]$ as the stronger gravitational field improves adiabaticity if all the other parameters in Eq. (10) remain the same. The improved adiabaticity results in a broader suppression pit in the survival probability and the *pp* neutrinos become more strongly suppressed for the same values of $\sin^2 2\theta_G$, which comes into conflict with the results from the gallium experiments.

Different components of the solar neutrino flux are suppressed differently in the two allowed regions. In the large mixing region the *pp* neutrinos are suppressed the least, by a factor of about 0.55–0.65. ^{7}Be, CNO and pep neutrinos are suppressed most strongly in the upper part of the allowed region and their suppression gradually decreases in the lower part of this region. The ^{8}B neutrinos are almost uniformly suppressed (by factors of 0.25 – 0.34) in the entire large mixing allowed region. In most of the allowed small mixing angle region the ^{7}Be neutrinos are suppressed more than the ^{8}B and the *pp* neutrinos. The lower part of the ^{8}B-neutrino spectrum ($E_\nu < 10$ MeV) is strongly suppressed and falls on the right (adiabatic) edge of the survival probability curve (see Fig. 1). The CNO and pep neutrinos are suppressed the most.

The relative suppression of the different solar neutrino fluxes is similar to the analogous regions in the case of a MSW solution for the mass mechanism. However, there is an important difference between the two cases: namely, the energy ranges corresponding to adiabatic and nonadiabatic transitions are opposite. It is this difference which leads to different neutrino spectra for the two cases. The nonadiabatic edge in the case of the mass mechanism is not as steep as the adiabatic edge in the case of the VEP mechanism. Since these are responsible for the spectral distortion of the boron neutrinos one expects more abrupt changes of this spectrum in the case of VEP.

B. Spectral distortion

It has been shown in [29] that the solar neutrino spectrum is independent of all solar model considerations to a very high accuracy. Distortions of the spectrum, if found experimentally, would constitute a strong evidence for a neutrino physics solution of the solar neutrino problem.

The Kamiokande II (KII) Collaboration has obtained the first piece of spectral information on solar neutrinos by measuring the energy spectrum of the recoil electrons from neutrino-electron scattering [30]. Because of the relatively large statistical errors, the constraints on possible distortions of the spectrum are not very stringent. We have used the KII data to rule out values of the parameters Δf and $\sin^2 2\theta_G$. The excluded region at 95% C.L. is shown as the hatched region in Fig. 2. This exclusion is obtained by comparing the predicted recoil-electron spectrum with the measured one for a large number of values for Δf and $\sin^2 2\theta_G$, taking into account the energy resolution and threshold efficiency function of the KII detector. The excluded region overlaps with part of the allowed "small mixing region" obtained from the χ^2 analysis of the event rates discussed above. It should be emphasized that, while the position and shape of the allowed regions in Fig. 2 depend on the predicted solar neutrino flux from the standard solar model, the region excluded by the recoil-electron spectrum is solar model independent.

The excluded region in Fig. 2 depends sensitively on the highest energy data point in the KII spectrum. This point has a relatively small error bar which is a result of combining the data from all higher-energy bins above 13 MeV. If this data point is ignored, we find that the excluded region will be reduced considerably and will no longer overlap with the allowed region. The situation will be improved when more precise measurements of the recoil-electron spectrum become available from the upcoming SNO and Super-Kamiokande detectors.

We have studied the possibility of using the SNO and Super-Kamiokande measurements to identify the mixing mechanism responsible for the solar neutrino problem. We show in Fig. 3 the predicted spectra for various allowed values of the mixing parameters. Spectra predicted for MSW transitions in the VEP mechanism and in the mass mechanism are displayed in Fig. 3(a) and Fig. 3(b), respectively. What is actually shown is the ratio of the predicted spectrum $F(T_e)$ to the corresponding spectrum $F_{\rm st}(T_e)$ calculated for the standard solar model [5] with no neutrino mixing. We normalize the value of this ratio such that it is equal to 1 for recoil electrons with energy $T_e = 10$ MeV. For large mixing angles, there is little distortion from the standard solar model spectrum, both for the VEP and for the mass mechanism. This is why the measured KII spectrum only excludes a region corresponding to small mixing angles (see Fig. 2). On the other hand, the spectral distortion for small mixing angles in the VEP case is noticeably different from that in the mass mechanism.

One possible measure of the difference in the spectral distortion is the derivative

$$\xi_e(T_e) = \frac{d}{dT_e}\left[\frac{F(T_e)}{F_{\rm st}(T_e)}\right]. \tag{18}$$

As an illustration of the sensitivity of this variable to the distortions of the shape of the spectral curves we have compared its values for the VEP and mass mechanisms

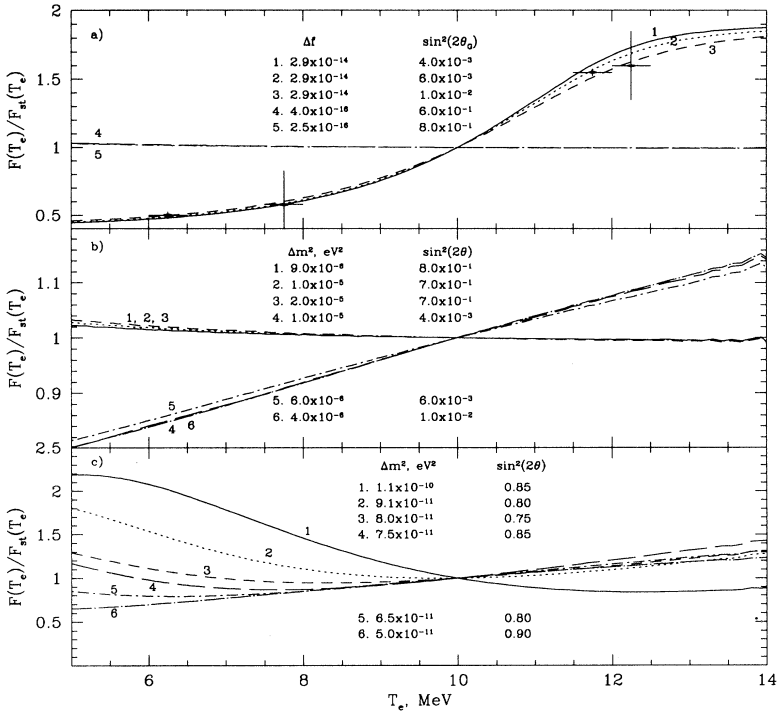

FIG. 3. Ratios of the predicted recoil-electron spectra for (a) "MSW-enhanced" VEP mechanism, (b) MSW effect in the mass mechanism, and (c) neutrino oscillations in vacuum (note the different scale in each of these cases) to the standard spectrum of recoil electrons from boron neutrinos. T_e is the recoil-electron energy. The chosen values of the parameters for each case correspond to values allowed by the current solar neutrino data. The two larger error bars represent the present experimental results and the other two are the estimated statistical errors after five years of data from the Super-Kamiokande detector.

at $T_e = 10$ MeV. For the VEP mechanism $\xi_e(10\ \text{MeV})$ is equal to 0.31, 0.29, and 0.27 MeV^{-1} for curves labeled from 1 to 3 in Fig. 3(a). In the case of the mass mechanism the corresponding values are 0.036, 0.035, and 0.044 MeV^{-1} for curves labeled 4 to 6 in Fig. 3(b). For the rest of the curves shown in these two figures the derivative is very close to zero, typically an order of magnitude smaller than the above values.

Since long-wavelength vacuum oscillation for the mass mechanism is still a possible solution to the solar neutrino problem, it is necessary to also study the calculated recoil-electron spectra for this case, which are shown in Fig. 3(c). We see that the spectral distortion here can be as large as that in the VEP mechanism. However, the character of this distortion is different. For curves labeled from 1 to 6 in Fig. 3(c) the corresponding values of $\xi_e(10\ \text{MeV})$ are -0.156, 0.0094, 0.057, 0.10, 0.089, and 0.0695 MeV^{-1}. Furthermore, at energies below 10 MeV the general behavior of the spectral distortion is drastically different in the two cases. Therefore future solar neutrino experiments should be able to distinguish, independent of solar model predictions of the neutrino fluxes, between the different scenarios by comparing the shapes of the recoil–electron spectra, provided the experimental uncertainties are sufficiently small.

In addition to neutrino-electron scattering, the SNO detector can also detect the ^{8}B neutrinos from the Sun by the process $\nu_e + d \rightarrow p + p + e^-$. In the case of the MSW effect for the mass mechanism the ^{8}B-neutrino spectrum is smoothly and almost uniformly distorted in the region between 5 and 14.5 MeV, which is the interval of energies to which the SNO detector is expected to be sensitive. On the other hand, in the case of the VEP mechanism, the distortion of the ^{8}B-neutrino spectrum is much more abrupt in the small mixing region. This is illustrated in Figs. 4(a) and 4(b) where the ^{8}B-neutrino spectra are shown in the two cases for sets of allowed parameters. Similar to Fig. 3, the spectra are normalized to the standard ^{8}B neutrino spectrum (corresponding to no neutrino mixing) and to their values at 10 MeV. It is evident from these figures that, for small mixing angles, the deviations from the standard ^{8}B-neutrino spectrum are large. Moreover, the spectral distortions in the case of the VEP mechanism are strikingly different from the corresponding ones in the case of the MSW solution for the mass mechanism. The derivative $\frac{d}{dE_\nu}[F(E_\nu)/F_{\text{st}}(E_\nu)]$ has values 1.1, 1.0, and 0.90 MeV^{-1} at $E_\nu = 10$ MeV for curves 1 to 3 in Fig. 4(a), whereas it is equal to 0.10, 0.093, and 0.10 MeV^{-1} for curves 4 to 6 in Fig. 4(b). The difference in the shape of these curves is big enough to be measured in the SNO detector as indicated by the estimated error bars after five years of operation of this detector.[2]

We also compare the VEP spectra with those predicted

[2]Efficiency and energy resolution have not been included in the estimate of the error bars. The error bars are simply the square root of the estimated number of events per year. Systematic errors due to spectrum broadening effects like three-body final state, Fermi motion, etc. have not been taken into account. These effects will have to be included in future more accurate studies.

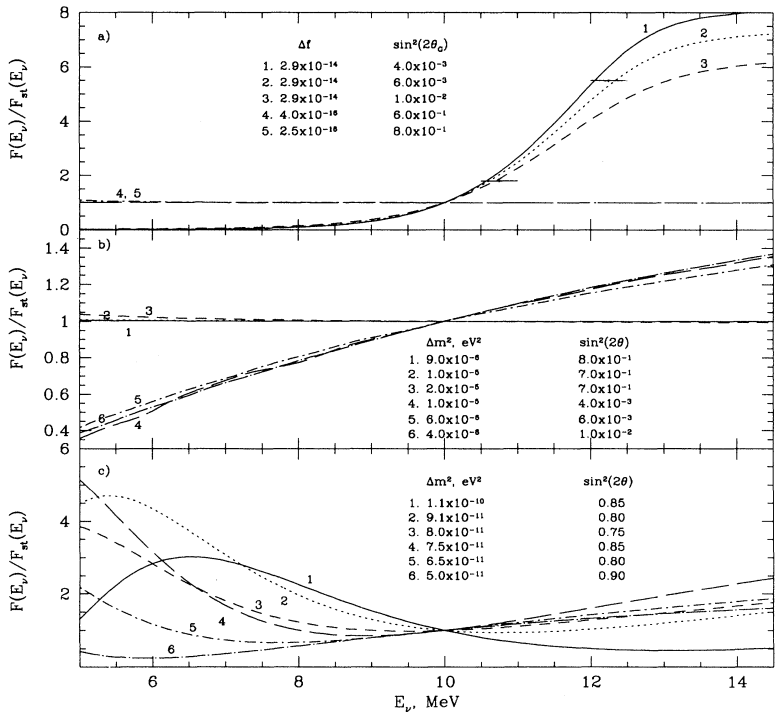

FIG. 4. Predicted ratios of ^{8}B-neutrino spectra to the standard boron-neutrino spectrum for the same three cases as in Fig. 3. Note the different scale used in each case. E_ν is the neutrino energy. The estimated statistical error bars after five years of operation of the SNO detector are also shown.

for the mass mechanism in the case of long-wavelength vacuum oscillations, displayed in Fig. 4(c). The values of the corresponding derivative at $E_\nu = 10$ MeV are – 0.43, – 0.16, 0.070, 0.23, 0.21, and 0.19 MeV^{-1} for curves labeled 1 to 6 in Fig. 4(c). We see again a measurable difference between the spectra in these two cases. The neutrino oscillations in vacuum result in stronger distortions in the lower spectrum of the energy interval between 5 and 14.5 MeV whereas the VEP distortions are more prominent at the higher energies.

IV. CONCLUSION

Using the current solar neutrino data, we find that the VEP mechanism can describe the data from the existing solar neutrino experiments. The existing data do, however, rule out a possible violation of the principle of equivalence for a substantial region of the Δf - $\sin^2 2\theta_G$ plane between $10^{-18} < \Delta f < 10^{-12}$. This result complements the constraints obtained from SN 1987A by comparing the arrival times of neutrinos and photons, $|f_\nu - f_\gamma| < 3 \times 10^{-3}$ [32,33], and by comparing neutrinos with anti-neutrinos, $|f_\nu - f_{\bar{\nu}}| < 10^{-6}$ [34,35]. It is also stronger than the best limit of 10^{-12} derived from torsion balance experiments [36], which refers to macroscopic samples of matter and not to neutrinos. Consequently, the violation of the equivalence principle by neutrinos, indicated by the allowed regions in Fig. 2, does not translate into a violation of the equivalence principle by the charged leptons at an unacceptable level. For example, it does not induce lepton flavor-changing transitions such as $\mu \to e\gamma$ at a rate already excluded by experiment [23].

If the violation of the equivalence principle has the gradient form given in Eq. (5) rather than the linear form of Eq. (4), then from Eq. (6) and the limits cited above for Δf, we conclude that a significant fraction of flavor-violating couplings in the range 10^{-3} eV $\lesssim M_f \lesssim 10^3$ eV are excluded.

Observation of the distortion of the solar neutrino spectrum would be a decisive proof [29] that neutrino physics is at the heart of the solar neutrino problem. We have shown that the recoil-electron spectrum measured by Kamiokande II excludes, in a solar model-independent way, a region of the otherwise allowed VEP parameter space. We have studied the prospects of using spectral measurements of solar neutrinos to distinguish among various neutrino oscillation mechanisms. In the case of small mixing angles, spectral measurements from upcoming solar neutrino experiments will be able to determine which is the underlying mechanism of neutrino mixing. On the other hand, atmospheric neutrino data favor large mixing, in which case spectral measurements of solar neutrinos cannot easily distinguish the VEP mechanism from the mass mechanism. In this case, long-baseline accelerator neutrino experiments [18,19] with typical neutrino energies between 1 and 20 GeV and separations of order hundreds of kilometers may provide the means to distinguish these two mechanisms.

ACKNOWLEDGMENTS

We are grateful to A. M. Polyakov for an informative and stimulating discussion of possible mechanisms for the

violation of the equivalence principle in string theories. J.N.B. acknowledges support from NSF Grant No. PHY 92-45317. The work of P.I.K. was partially supported by the Institute for Advanced Study. He would like to thank the Theory Group at Fermilab. C.N.L. thanks the International School for Advanced Studies, especially S. T. Petcov, for their hospitality during the latter stage of this work and also S. T. Petcov and A. Yu Smirnov for useful discussions. This work was supported in part by the U.S. Department of Energy under Grant Nos. DE-FG05-85ER-40219 and DE-FG02-84ER40163 and by the North Carolina Supercomputing Program.

APPENDIX A: ADIABATICITY CONDITION

The adiabaticity condition, Eq. (10), is given for the case of massless neutrinos. In [21] this condition has been given for massive neutrinos but for the specific case of an exponential electron number density. Here we derive the most general expression for the adiabaticity condition for massive neutrinos valid for any gravitational potential and any electron number density distribution. The limit of massless neutrinos considered in the text can be obtained simply by putting $\Delta m^2 = 0$. Our derivation follows closely the one in [37] for the case of MSW transitions.

The evolution equation, Eq. (11), for neutrinos propagating in matter can be written in an equivalent form as a system of coupled first order differential equations for the probability amplitudes $A_e(r)$ and $A_\mu(r)$ to find, respectively, an electron and a μ neutrino at a distance r from the production point of an electron neutrino:

$$i\frac{d}{dr}\begin{pmatrix} A_e \\ A_\mu \end{pmatrix} = \begin{bmatrix} 0 & b(r) \\ b(r) & a(r) \end{bmatrix}\begin{pmatrix} A_e \\ A_\mu \end{pmatrix}. \tag{A1}$$

For massive neutrinos the elements of the evolution matrix read

$$a(r) = -\sqrt{2}G_F N_e(r) - 2E\phi(r)\Delta f\cos 2\theta_G + \frac{\Delta m^2}{2E}\cos 2\theta, \tag{A2}$$

$$b(r) = -E\phi(r)\Delta f\sin 2\theta_G + \frac{\Delta m^2}{4E}\sin 2\theta. \tag{A3}$$

In the adiabatic approximation, Eq. (A1) can be diagonalized at any fixed distance r with the help of a distance-dependent orthogonal matrix

$$\begin{pmatrix} A_e \\ A_\mu \end{pmatrix} = \begin{bmatrix} \cos\omega(r) & -\sin\omega(r) \\ \sin\omega(r) & \cos\omega(r) \end{bmatrix}\begin{pmatrix} B_e \\ B_\mu \end{pmatrix}. \tag{A4}$$

This orthogonal transformation preserves the total probability $|A_e|^2+|A_\mu|^2 = |B_e|^2+|B_\mu|^2$. The evolution equation takes the form

$$i\frac{d}{dr}\begin{pmatrix} B_e \\ B_\mu \end{pmatrix} = \left[\begin{pmatrix} M_1 & 0 \\ 0 & M_2 \end{pmatrix} - \begin{pmatrix} \cos\omega(r) & \sin\omega(r) \\ -\sin\omega(r) & \cos\omega(r) \end{pmatrix} \times i\frac{d}{dr}\begin{pmatrix} \cos\omega(r) & -\sin\omega(r) \\ \sin\omega(r) & \cos\omega(r) \end{pmatrix}\right]\begin{pmatrix} B_e \\ B_\mu \end{pmatrix}, \tag{A5}$$

where M_1 and M_2 are the eigenvalues of the evolution matrix:

$$M_{1,2} = \frac{a \pm \sqrt{(a^2+4b^2)}}{2}. \tag{A6}$$

From the diagonalization condition it follows also that

$$\omega(r) = -\frac{1}{2}\arctan\left(\frac{2b}{a}\right). \tag{A7}$$

The evolution of the neutrino state is adiabatic if the nondiagonal terms of the evolution matrix in Eq. (A5) are much smaller than the diagonal ones. This condition can be written explicitly as

$$\frac{|b'a - ba'|}{a^2+4b^2} \ll \frac{\sqrt{a^2+4b^2}-a}{2}. \tag{A8}$$

At the resonance ($a = 0$) this condition reads

$$\kappa = \frac{4b^2}{|a'|} \gg 1. \tag{A9}$$

Substituting here the expressions for $a(r)$ and $b(r)$ from Eqs. (A2) and (A3), one obtains the most general adiabaticity condition for the VEP mechanism, including neutrino masses, which is valid for an arbitrary gravitational potential and electron number density:

$$\kappa = \left|\frac{(2E\phi\Delta f\sin 2\theta_G - \frac{\Delta m^2}{2E}\sin 2\theta)^2}{2E\phi\Delta f\cos 2\theta_G\left[\frac{N_e'}{N_e} - \frac{\phi'}{\phi}\right] - \frac{N_e'}{N_e}\frac{\Delta m^2}{2E}\cos 2\theta}\right|_{\rm res} \gg 1. \tag{A10}$$

APPENDIX B: ANALYTIC DESCRIPTION OF NEUTRINO CONVERSION IN THE VEP MECHANISM

We explain in this appendix how Eq. (17) has been derived and the accuracy with which it approximates the average survival probability. The evolution equation in the VEP mechanism, Eq. (A1), differs from the corresponding one for the MSW mechanism, most notably by the dependence of the nondiagonal terms in the evolution matrix on the distance. For b = const, the equivalent second order equation, Eq. (11), has the same form as the corresponding second order equation in the MSW case

and can be solved exactly in the same way [38], e.g., for the case of an exponential electron number density distribution. The resulting analytical solution in terms of the confluent hypergeometric function converges to Eq. (17) both in the adiabatic and nonadiabatic limits, as shown in [26] for MSW transitions. A derivation of an exact analytical solution of Eq. (11) with $b \neq$ const might still be possible for some specific gravitational potentials. However, a simple observation is enough to convince oneself that the approximate analytical solution, Eq. (17), will be almost exact in most of the parameter range relevant for solar neutrinos. Inside the Sun the gravitational potential changes slowly from 10^{-5} at the center to 2×10^{-6} at the surface and the term $|b'/b|$ is of order $R_\odot{}^{-1}$. In contrast $|a| \gg 1/R_\odot$ up to densities smaller than $0.01 N_A/\mathrm{cm}^3$, where N_A is the Avogadro number. These densities occur at distance $r > 0.93R_\odot$ where no significant transitions can take place. Therefore, $|b'/b| \ll |a|$ everywhere except in the resonance region where $a = 0$. In this case, if the nondiagonal terms were constant, this system would describe oscillations with maximal amplitude. Because of the dependence on r the oscillations are damped. It can be easily shown that the damping will be negligible if $|b'/b| \ll |b|$. This gives the condition

$$|b(r)|R_\odot = 7\times10^{15}\Delta f\left(\frac{E}{\mathrm{MeV}}\right)\sin(2\theta_G) \gg 1, \quad \text{(B1)}$$

where we have used the smallest value, 2×10^{-6}, for the gravitational potential in the Sun. It follows that, for $\Delta f(\frac{E}{\mathrm{MeV}}) > 10^{-16}/\sin(2\theta_G)$, the dependence of b on the distance can be neglected and the evolution equation for the VEP mechanism can be solved in the same way as the corresponding equation for the MSW mechanism.

In addition to the above argument, as stated in the text, we have checked the accuracy of the analytical description of the neutrino survival probability by numerically integrating the evolution equations and comparing the results so obtained with the results given by Eq. (17). As explained in [26] for the case of MSW transitions, in order for the latter equation to give a sufficiently accurate approximation to the survival probability, a running adiabaticity parameter has to be used which changes with the resonance point for different values of E and Δf [see Eq. (9)]. With the incorporation of such a running adiabaticity parameter the analytic description was found to be accurate within a few percent even in the region where according to the above estimate Eq. (17) would fail.

[1] R. Davis, D.S. Harmer, and K.C. Hoffman, Phys. Rev. Lett. **20**, 1205 (1968); R. Davis, Jr., in *Cosmic Ray Conference*, Proceedings of the 23rd International Conference, Calgary, Canada, 1993, edited by R. Hicks *et al.* (World Scientific, Singapore, 1994); Prog. Nucl. Part. Phys. **32**, 13 (1994); K. Lande, in *Neutrino 94*, Proceedings of the 16th International Conference on Neutrino Physics and Astrophysics, Eilat, Israel, edited by A. Dar, G. Eilam, and M. Gronau [Nucl. Phys. B (Proc. Suppl.) **38** (1995)].

[2] Kamiokande II Collaboration, K. Hirata *et al.*, Phys. Rev. Lett. **65**, 1297 (1990); **65**, 1301 (1990); Phys. Rev. D **44**, 2241 (1991); the latest solar neutrino result is given by Y. Suzuki, in *TAUP'93*, Proceedings of the Third International Workshop on Theoretical and Phenomenological Aspects of Underground Physics, Assergi, Italy, 1993, edited by C. Arpesella, E. Bellotti, and A. Bottino [Nucl. Phys. B (Proc. Suppl.) **35** (1994)].

[3] SAGE Collaboration, J.N. Abdurashitov *et al.*, Phys. Lett. B **328**, 234 (1994); A.I. Abazov *et al.*, Phys. Rev. Lett. **67**, 3332 (1991); V.N. Gavrin, Talk given at the International Symposium "Neutrino Telescopes," Venice, 1994.

[4] GALLEX Collaboration, P. Anselmann *et al.*, Phys. Lett. B **327**, 377 (1994); **314**, 445 (1993); **285**, 376 (1992); **285**, 390 (1992).

[5] J.N. Bahcall and M.M. Pinsonneault, Rev. Mod. Phys. **64**, 885 (1992).

[6] J.N. Bahcall and R.K. Ulrich, Rev. Mod. Phys. **60**, 297 (1989).

[7] I.-J. Sackman, A.I. Boothroyd, and W.A. Fowler, Astrophys. J. **360**, 727 (1990).

[8] V. Castelani, S. DeglInnocenti, and G. Fiorentini, Astron. Astrophys. **271**, 601 (1993).

[9] S. Turck-Chieze and I. Lopez, Astrophys. J. **408**, 347 (1993); S. Turck-Chieze *et al.*, Phys. Rep. **230**, 57 (1993).

[10] G. Berthomieu, J. Provost, P. Morel, and Y. Lebreton, Astron. Astrophys. **268**, 775 (1993).

[11] A. Kovetz and G. Shaviv, Astrophys. J. **426**, 787 (1994).

[12] C.R. Proffitt, Astrophys. J. **425**, 849 (1994).

[13] J. Christensen-Dalsgaard, Europhys. News **25**, 71 (1994).

[14] J.N. Bahcall and H. Bethe, Phys. Rev. D **47**, 1298 (1993); Phys. Rev. Lett. **65**, 2233 (1990).

[15] B.M. Pontecorvo, Zh. Eksp. Teor. Fiz. **34**, 247 (1958) [Sov. Phys. JETP **7**, 172 (1958)]; see also Z. Maki, M. Nakagawa, and S. Sakata, Prog. Theor. Phys. **28**, 870 (1962).

[16] L. Wolfenstein, Phys. Rev. D **17**, 2369 (1978); **20**, 2634 (1979); S.P. Mikheyev and A.Yu Smirnov, Yad. Fiz. **42**, 1441 (1985) [Sov. J. Nucl. Phys. **42**, 913 (1985)]; Nuovo Cimento **C9**, 17 (1986).

[17] M. Gasperini, Phys. Rev. D **38**, 2635 (1988); **39**, 3606 (1989); see also A. Halprin and C.N. Leung, Phys. Rev. Lett. **67**, 1833 (1991); in *TAUP'91*, Proceedings of the Second International Workshop on Theoretical and Phenomenological Aspects of Underground Physics, Toledo, Spain, edited by A. Morales, J. Morales, and J. Villar [Nucl. Phys. B (Proc. Suppl.) **28A**, 139 (1992)].

[18] J. Pantaleone, A. Halprin, and C.N. Leung, Phys. Rev. D **47**, R4199 (1993).

[19] K. Iida, H. Minakata, and O. Yasuda, Mod. Phys. Lett. A **8**, 1037 (1993).

[20] M.N. Butler, S. Nozawa, R. Malaney, and A.I. Boothroyd, Phys. Rev. D **47**, 2615 (1993).

[21] H. Minakata and H. Nunokawa, Phys. Rev. D **51**, 6625 (1995).

[22] A. Halprin, C.N. Leung, and J. Pantaleone, in *Weak Interactions and Neutrinos*, Proceeding of the 14th Inter-

national Workshop, Seoul, Korea, 1993, edited by J. E. Kim and S. K. Kim (World Scientific, Singapore, 1994).
[23] A. Halprin, C.N. Leung, and J. Pantaleone (in preparation).
[24] P. Morrison, Am. J. Phys. **26**, 358 (1958); M.L. Good, Phys. Rev. **121**, 311 (1961); I.R. Kenyon, Phys. Lett. B **237**, 274 (1990); R.J. Hughes and M.H. Holzscheiter, J. Mod. Opt. **39**, 263 (1992); R.J. Hughes, Phys. Rev. D **46**, R2283 (1992).
[25] For a recent discussion of the violation of the equivalence principle in superstring theories, see T. Damour and A. M. Polyakov, Nucl. Phys. **B423**, 532 (1994).
[26] S.T. Petcov, Phys. Lett. B **200**, 373 (1988); **214**, 139 (1988); see also *Weak Interactions and Neutrinos*, Proceedings of the International Conference, Ginosar, Israel, 1989, edited by P. Singer and B. Gad Eilam [Nucl. Phys. B (Suppl.) **13**, 527 (1990)]; P. I. Krastev and S.T. Petcov, Phys. Lett. B **207**, 64 (1988).
[27] N. Hata and P. Langacker, Phys. Rev. D **50**, 632 (1994).
[28] P.I. Krastev and S.T. Petcov, "Testing the Vacuum Oscillation and the MSW Solutions of the Solar Neutrino Problem," Report No. FERMILAB–PUB–94/188–T, 1994, hep-ph/9408234 (unpublished).
[29] J.N. Bahcall, Phys. Rev. D **44**, 1644 (1991).
[30] K.S. Hirata *et al.*, Phys. Rev. Lett. **65**, 1301 (1990).
[31] K.S. Hirata *et al.*, Phys. Rev. D **44**, 2241 (1991).
[32] M.J. Longo, Phys. Rev. Lett. **60**, 173 (1988).
[33] L.M. Krauss and S. Tremaine, Phys. Rev. Lett. **60**, 176 (1988).
[34] J.M. LoSecco, Phys. Rev. D **38**, 3313 (1988).
[35] S. Pakvasa, W.A. Simmons, and T.J. Weiler, Phys. Rev. D **39**, 1761 (1989).
[36] V.B. Braginsky and V.I. Panov, Zh. Eksp. Teor. Fiz. **61**, 873 (1971) [Sov. Phys. JETP **34**, 463 (1972)].
[37] S.P. Mikheyev and A.Yu. Smirnov, Zh. Eksp. Teor. Fiz. **92**, 404 (1987) [Sov. Phys. JETP **65**, 230 (1987)].
[38] T. Kaneko, Prog. Theor. Phys. **78**, 532 (1987); S. Toshev, Phys. Lett. B **196**, 170 (1988); M. Ito, T. Kaneko, and M. Nakagawa, Prog. Theor. Phys. **79**, 13 (1988); S.T. Petcov, Phys. Lett. B **200**, 373 (1988).